Current Research in Food Science 10 (2025) 100978

Contents lists available at ScienceDirect

Current Research in Food Science

journal homepage: www.sciencedirect.com/journal/current-research-in-food-science

Ginsenosides 20R-Rg3 and Rg5 enriched black ginseng inhibits colorectal cancer tumor growth by activating the Akt/Bax/caspase-3 pathway and modulating gut microbiota in mice

Peng Yu [a,1], Weiyin Xu [a,1], Yanqi Li [b], Zhaoyang Xie [b], Simeng Shao [b], Jianing Liu [a], Ying Wang [c], Long Wang [b], Hongmei Yang [b,*]

[a] College of Pharmacy, Changchun University of Chinese Medicine, Changchun, 130117, China
[b] Public Experimental Center, Changchun University of Chinese Medicine, 130117, Changchun, China
[c] School of Medicine, Changchun Institute of Science and Technology, Changchun, 130600, China

ARTICLE INFO

Keywords:
Anti-apoptosis
Black ginseng
Colorectal cancer
Rare ginsenosides
Gut microbiota

ABSTRACT

Black ginseng (BG) is of great interest for its anti-cancer property. Its detailed mechanism, however, is still lacking. This study aims to evaluate the effectiveness of ginsenosides 20R-Rg3 and Rg5 enriched BG (Rg3/Rg5-BG), innovatively prepared by low temperature steam-heating process, against colorectal cancer (CRC), and elucidate its potential molecular mechanism. Interestingly, much higher concentrations of rare ginsenosides were detected in this unique BG than those in red ginseng, especially 20R-Rg3 and Rg5, which may contribute to treatment of CRC. As expected, Rg3/Rg5-BG demonstrated a dose-dependent reduction in cancer cell viability, along with the induction of cell apoptosis and cell cycle arrest. Moreover, Rg3/Rg5-BG retarded tumor growth in the model mice, as evidenced by downregulation of anti-apoptotic Bcl-2 protein and phosphatidyl Akt, and upregulation of the apoptotic proteins Bax, caspase-8, and cleaved caspase-3, enhancing apoptosis of tumor cells. Additionally, Rg3/Rg5-BG treatment improved the gut microbiota and intervened with bacteria associated with cancer development, including increasing beneficial probiotics such as *Candidatus_Saccharibacteria* and *Saccharibacteria_genera_incertae_sedis* and decreasing pernicious bacteria (*Vampirovibrio*, *Clostridium_XlVb*, etc.). Our results manifested for the first time that Rg3/Rg5-BG exerted its anti-cancer effects: through activation of the caspase-3/Bax/Bcl-2 pathway and by altering the gut microbiome composition, thus paving the way for new therapeutic strategies that incorporate natural products in cancer treatment.

1. Introduction

Colorectal cancer (CRC) significantly adds to global cancer fatalities as a prevalent digestive tract malignancy (Siegel et al., 2019). Treatment modalities for colorectal cancer encompass chemotherapy, radiotherapy, surgical intervention, targeted therapy, and immunotherapy (Miller et al., 2016). Despite progress, mortality and morbidity rates are still high. CRC involves complex interactions of genetic and environmental factors with diverse mechanisms (Brenner et al., 2014). Understanding these molecular mechanisms is crucial for developing effective treatments. Gut inflammation, diet, and the enteric microbiota significantly influence CRC progression (Tilg et al., 2018), revealing notable distinctions in gut microbiota between CRC patients and healthy individuals (Gagnière et al., 2016).

Chemotherapy drugs for CRC, for example 5-fluorouracil (5-FU), often induce side effects including diarrhea, bone marrow suppression, and heart toxicity (Focaccetti et al., 2015). Natural products have emerged as highly promising candidates owing to their potent anti-cancer properties and minimal adverse effects (Ekiert and Szopa, 2020) Ginseng, a traditional herbal medicine from East Asia, is renowned for its medicinal properties, which can significantly reduce the incidence of various cancers such as lung and CRC (Saeed et al., 2022; Yun and Choi, 1998). Ginsenosides such as Rg3, compound K, and Rh2 have been shown to inhibit the proliferation of CRC cell lines (He et al., 2011; Liu et al., 2018; Phi et al., 2018; Yang et al., 2016). Ginsenosides have the potential to diminish the expression of proliferating

* Corresponding author. The Public Experimental Center, Changchun University of Chinese Medicine, Changchun, 130117, China.
E-mail address: yanghm0327@sina.cn (H. Yang).
[1] These authors contributed equally to this work.

https://doi.org/10.1016/j.crfs.2025.100978
Received 30 September 2024; Received in revised form 7 January 2025; Accepted 17 January 2025
Available online 20 January 2025

cell nuclear antigen (He et al., 2011) and enhance the growth of beneficial gut bacteria (Chen et al., 2016).

Ginseng has been used in China as a medicinal herb for thousands of years. In recent years, a variety of ginseng products have been used as raw materials for functional foods, mainly including red ginseng (RG) and black ginseng (BG). The color of red ginseng obtained after steaming changes from yellowish-white to reddish-brown, and the texture gradually changes from hard to soft (Huang et al., 2022). Besides the changes in its characteristics, the chemical composition of RG has also undergone significant alterations. Regular ginseng contains almost no rare ginsenosides, while RG has a concentration of 0.243 % of these rare compounds, which explains, to some extent, why the nutritional value of red ginseng is greater than that of regular ginseng (Jin et al., 2015). BG is a newly processed type of ginseng that is created from fresh ginseng using various techniques such as steaming, fermenting, and puffing technology (Huang et al., 2023). It is noteworthy that the steaming process causes significant changes in the type and number of secondary metabolites in ginseng, including ginsenosides and carbohydrates (Zhu et al., 2019), which can greatly change its pharmacological activity (Metwaly et al., 2019). BG contains more rare ginsenosides such as Rk1 and Rg5, exhibiting more potent biological activities including anti-cancer effects than both white ginseng and red ginseng (Chen et al., 2017; Metwaly et al., 2019). Currently, there is a lack of in-depth research about the effects of ginsenosides in BG on CRC and the detailed molecular mechanisms.

Here, the goal of the current study was to examine the anti-cancer properties of the total ginsenosides from black ginseng (Rg3/Rg5-BG), innovatively prepared by a low-temperature steam-heating process, in CRC, along with the underlying molecular mechanisms. We performed the chemical composition of Rg3/Rg5-BG by UPLC-MS/MS technology and the anticancer effects both in vitro and in vivo. Finally, we investigated apoptosis and gut microbiota, critical factors in CRC pathogenesis, following Rg3/Rg5-BG administration to model mice. This study lays the groundwork for potentially developing Rg3/Rg5-BG as an adjunctive therapy for CRC treatment.

2. Materials and methods

2.1. Materials

All the standards of ginsenosides and 5-FU with purities over 98.0 % were purchased from Shanghai Yuanye Biotechnology Co., Ltd (Shanghai, China). All the antibodies, and the anti-goat IgG secondary antibody were bought from Wanlei Biotechnology Co., Ltd. (Shenyang, China). Acetonitrile, methanol, and formic acid were obtained from Fisher Chemical (Pittsburgh, PA, USA). Huangshi Research Biotechnology Co., Ltd. (Hubei, China) supplied the multi-Analyte ELISArray Kits for inflammatory cytokine analysis. Cell counting kit 8 (CCK8) was obtained from Invigentech (Murphy Ave, Irvine, USA). BD Biosciences (San Diego, CA, USA) supplied the FITC-Annexin V and propidium iodide (PI) apoptosis kit. Bio-Rad (Hercules, CA, USA) provided the enhanced chemiluminescence (ECL) Western blotting (WB) detection kit. Roche Ltd. (Basel, Switzerland) supplied the TUNEL assay kit.

2.2. Preparation of Rg3/Rg5-BG and UPLC-MS/MS

Ginsenosides from BG, processed from five-year-old ginseng bought in the Wanliang Market (Jilin, China) at 70 °C and 70 % relative humidity for 19 days, were extracted using a 70 % methanol solution and prepared for MS analysis according to the previous research (Wei et al., 2023).

The AB SCIEX QTRAP® 6500 mass spectrometer, equipped with a Turbo Ion Spray source using electrospray ionization (ESI) in multiple reaction monitoring (MRM) negative-ion mode, was employed for the detection of Rg3/Rg5-BG. The parameters for the ESI source were optimized and preset for consistent measurements as follows: source temperature, 350 °C; curtain gas, 30 psi; sheath gas, 50 psi; drying gas, 50 psi; spray voltage, 4500 V. The mass spectrometer's parameters were optimized using Analyst 1.6.2 software to enhance sensitivity for all analytes, with further details provided in Table 1.

Analytes were separated using an ExionLC AD liquid chromatography system from AB SCIEX, USA, on a Hypersil GOLD™ C18 column (100 mm × 2.1 mm i. d., 1.9 μm particle size, Thermo Scientific) at a flow rate of 0.25 mL/min and a column temperature of 35 °C. The gradient solvent system consisted of solvent A (0.1 % formic acid in water) and solvent B (acetonitrile). The gradient profile was as follows: starting at 18 % B, increasing to 45 % B at 10 min, 50 % B at 18 min, 52 % B at 20 min, reaching 90 % B at 25 min, and returning to 18 % B at 26 min.

Table 1
The MRM data and standard curve of the analytes.

Ginsenosides	Q1/Q3	DP (V)	CE (V)	Standard curve	R^2	Linear range (ng/mL)
Ro	955.5/793.5	−60	−30	y = 971.5x + 38.8	0.9993	0.5–130.0
Rb1	1077.4/783.5	−240	−64	y = 3257.3x + 822.0	0.9996	0.6–560.0
Rb2	1123.6/1077.7	−60	−30	y = 3244.5x - 834.5	0.9995	1.0–500.0
Rb3	1123.6/1077.6	−280	−30	$y = 8.9e^4x$ - 171.1	0.9970	1.0–500.0
Rc	945.6/783.8	−277	−65	$y = 4.0e^4x$ + 7619.3	0.9969	0.6–570.0
Rd	991.5/637.4	−60	−65	y = 899.7x + 357.0	0.9959	0.6–1140.0
Re	845.5/637.4	−60	−50	y = 5002.6x + 185.2	0.9980	0.5–760.0
Rf	637.4/475.3	−225	−35	$y = 1.8e^4x$ - 2383.2	0.9974	0.5–1000.0
F1	667.5/459.5	−190	−55	y = 4220.3x - 171.4	0.9978	0.5–125.0
CK	683.4/475.4	−60	−46	y = 1346.4x - 151.2	0.9960	0.5–125.0
20R-Rh1	683.4/475.4	−65	−45	y = 6008.6x + 46.6	0.9929	0.5–225.0
20S-Rh1	665.4/619.4	−42	−25	y = 5842.1x - 80.3	0.9993	0.4–218.8
Rh4	811.5/765.7	−60	−29	$y = 7.9e^3x$ + 1065.4	0.9960	0.5–966.7
Rk1	1077.4/783.5	−240	−64	$y = 1.4e^5x + 1.68e^4$	0.9996	0.5–525.0
Rk3	665.4/619.4	−70	−27	$y = 4.1e^4x$ + 2090.3	0.9994	0.5–237.5
Rg2	829.5/475.4	−66	−60	$y = 2.2e^4x$ - 68.7	0.9953	0.5–525.0
20S-Rg3	829.5/783.5	−71	−31	$y = 2.8e^5x$ – 6150.0	0.9974	0.5–1000.0
20R-Rg3	829.5/783.5	−50	−32	$y = 3.3e^4x + 1.2e^4$	0.9977	5.5–700.0
Rg5	811.4/765.4	−230	−35	$y = 1.8e^4x$ + 913.4	0.9987	0.4–720.0
Rg6	811.4/765.4	−27	−30	$y = 3.4e^4x$ - $1.2e^4$	0.9976	0.5–500.0

2.3. Cell culture and cell viability

The CRC cell lines HCT-116, derived from humans, and CT26, originating from mice (iCell Bioscience Inc., Shanghai, China), were cultured in McCoy's 5A medium and RPMI-1640 medium (Gibco-Life Technologies), respectively, supplemented with 10 % fetal bovine serum (Sigma-Aldrich) and 1 % penicillin/streptomycin (Invitrogen, Life Technologies). Cell proliferation was evaluated via the CCK8 kit (Murphy Ave. Irvine, USA), following the manufacturer's protocol. The cells were confirmed mycoplasma-free and authenticated by Genewiz, Inc. (Suzhou, China) and Genetic Testing Biotechnology, Inc. (Suzhou, China) using the short tandem repeat method. They were cultured in a humidified incubator at 37 °C with 5 % CO_2.

As for the viability determination, HCT-116 and CT26 (1×10^3) suspended in 200 μL medium were seeded in triplicate in a 96-well plate and cultured at 37 °C until reaching 80 % confluence. Cells from each cell line were treated with varying concentrations of Rg3/Rg5-BG (0, 2.7, 2.9, 3.1, 3.3, 3.5 mg/mL), (0, 1.5, 1.7, 1.9, 2.1, 2.3 mg/mL), and 5-FU (0, 5, 6.25, 12.5, 25 μg/mL) for 24 h, respectively. As controls, cells were treated in triplicate with medium and then incubated at 37 °C for 2 h after replacing the original medium with 10 % CCK8-containing medium. Absorbance at 450 nm was assayed using a microplate reader (Bio-Tek, USA).

2.4. Flow cytometry assay and cell cycle analysis

Following a 24-h exposure of each cell line to Rg3/Rg5-BG and 5-FU, as well as to medium-treated controls, cell apoptosis was evaluated utilizing the Annexin V FITC apoptosis detection kit (BD Co., USA), in accordance with the manufacturer's guidelines. Cell percentages were determined using the Merck Guava EasyCyte flow cytometer system (Darmstadt, Germany) and analyzed with FlowJo software. Cells were plated in 6-well plates, allowed to grow overnight, and treated in triplicate with Rg3/Rg5-BG (3.0 mg/mL in HCT116 cells, 1.7 mg/mL in CT26 cells), 5-FU (12.5 μg/mL in both cells), and medium. Treatments were maintained for up to 48 h, and each well was collected into individual flow tubes. Collected cells were fixed by adding 1 mL of 70 % ethanol and kept at 4 °C overnight. After centrifugation, cells were washed twice with cold 1 × PBS and stained with PI solution (50 μg/mL PI in H_2O, 0.1 % Triton-X 100, 0.1 % trisodium citrate dehydrate, 6.25 μg/mL RNaseA) for 30 min at 37 °C. DNA content was subsequently analyzed using flow cytometry (NovoCyte, 2000; Agilent, USA), with a minimum of 20,000 cells analyzed per sample.

2.5. In vivo study of xenograft growth in nude mice

The Changchun University of Chinese Medicine Institutional Animal Care and Use Committee approved the animal use protocol (No.2023283). Thirty female BALB/c mice, aged 5–6 weeks and weighing between 18 and 20 g, were procured for the study. 1×10^6 CT26 cells were subcutaneously transplanted into the left axillary region of each of the 30 mice. After 10–12 days of allowing the tumors to establish, a 3-week treatment period was initiated when a tumor size of 100 mm^3 was reached. The mice were randomly assigned to one of the three groups: Group 1 received water orally (tumor control), Group 2 received a weekly intraperitoneal injection of 30 mg/kg 5-FU (positive control), and Group 3 received daily oral treatment with Rg3/Rg5-BG at 30 mg/kg. Tumor growth was assessed biweekly using a digital caliper, and tumor volume was calculated using the formula: length × $width^2$ × 0.5.

2.6. ELISA analysis

Blood harvested from mouse eyeballs was permitted to clot at room temperature for 2 h, after which it was centrifuged at 1000 g for 20 min. The supernatants were assayed for interleukin-2 (IL-2) and tumor necrosis factor-α (TNF-α) using ELISA kits (Hubei Huangshi Biotechnology Co., Ltd., China) according to the manufacturer's instructions, measuring absorbance at 450 nm.

2.7. Western blot

The protein concentration of each sample was assessed using a BCA protein assay kit from Beyotime Biotechnology, China. A quantity of 20 μg of protein was subjected to separation on 12 % SDS-PAGE gels, followed by a transfer to PVDF membranes (0.45 mm, Merck Millipore). The membranes were then blocked and incubated overnight at 4 °C with the primary antibodies. The next day, membranes were treated with an HRP-conjugated secondary antibody at room temperature for 1 h. Signals were discerned employing an ECL detection kit and visualized utilizing the Bio-Rad ChemiDoc MP imaging system.

2.8. Histological assessment and TUNEL staining

Xenograft tumors were harvested and embedded in paraffin blocks, with tissue sections cut at 4 μm for hematoxylin & eosin (H&E) staining. Tumor specimens were preserved in 4% paraformaldehyde for 24 h, subsequently embedded in paraffin, and sectioned into 5 μm slices for TUNEL staining, employing assay kits in accordance with the manufacturer's guidelines. Images were captured using confocal microscopy (Olympus, Japan).

2.9. Fecal DNA extraction and 16s RNA sequencing-based phylogenetic analysis

The TopTaq DNA Polymerase kit by Transgen (China) was utilized to extract DNA from the mouse fecal samples frozen in liquid nitrogen based on the provided guidelines. Amplification and sequencing of the V3-V4 variable region of 16S rDNA gene from the bacteria were performed using the Illumina MiSeq Benchtop Sequencer (Illumina, USA) to produce outcomes founded on sequenced reads and operational taxonomic units (OTUs) with a 97 % similarity threshold.

2.10. Statistical analysis

Mean ± standard deviation (SD) is presented for data analysis. Repeated measures ANOVA and Student's t-tests were conducted, with at least three replicates. Statistical analyses were performed utilizing GraphPad Prism 9.4.1 software (GraphPad, San Diego, CA, USA).

3. Results

3.1. Abundant rare ginsenosides were detected in Rg3/Rg5-BG extracts

In order to ascertain the active compounds, a total of 20 ginsenosides, including the 12 rare ginsenosides CK, 20R-Rh1, 20S-Rh1, F1, Rh4, Rk1, Rk3, Rg2, 20S-Rg3, 20R-Rg3, Rg5, Rg6, were examined. The contents of 20 ginsenosides in BG and RG extracts are presented in Fig. 1A.

Evidently, the contents of total rare ginsenosides (TRG) were much higher than those of total common ginsenosides (TCG) in BG (Fig. 1A). More remarkably, the content of TRG in BG was much higher (13.7 times) than that in RG. Interestingly, from Fig. 1B, it is clearly seen that the contents of rare ginsenosides 20R-Rg3, Rg5, Rk1, and Rh4 in BG are much more than those in RG as shown in Fig. 1B. Hence, it was speculated that BG may have relatively good anticancer effects.

3.2. Rg3/Rg5-BG reduced cell viability and induced apoptosis in HCT116 and CT26 cells

Firstly, cell viability was evaluated so as to test the effect of Rg3/Rg5-BG on CRC cells. As manifested in Fig. 2A and B, the cell viability

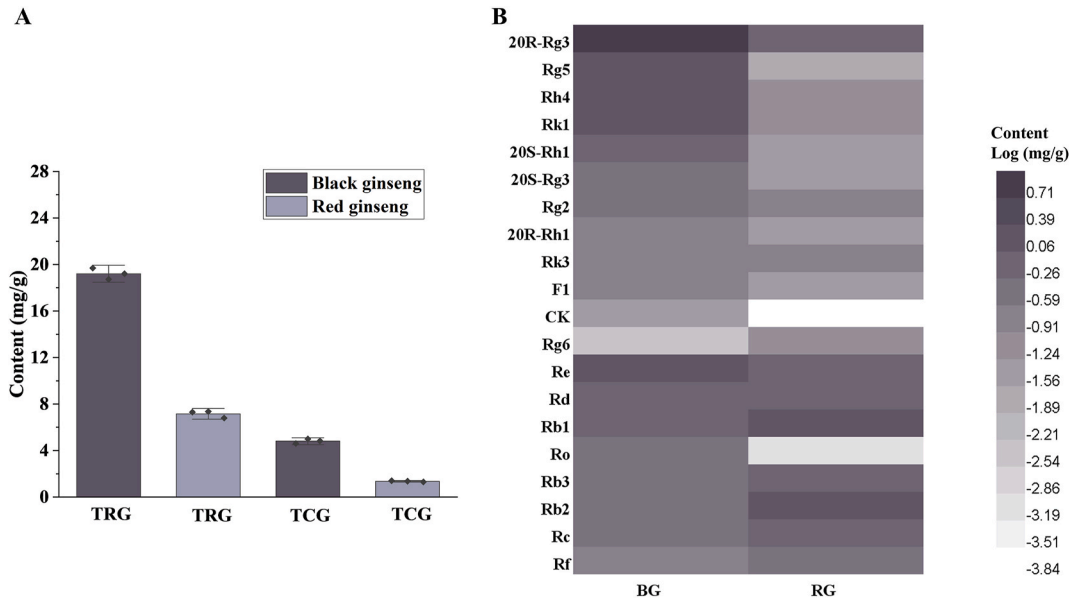

Fig. 1. (A) The contents of the total ginsenosides in BG and RG (n = 3, RSD ≤3%). (B) Heatmap of the 20 ginsenosides. Each ginsenoside is represented by a colored box reflecting the content expressed as mg/g.

decreased with increasing Rg3/Rg5-BG concentration in CCK8 experiments in a dose-dependent manner, revealing that Rg3/Rg5-BG inhibited the growth of CRC cells. The IC50 value of Rg3/Rg5-BG was determined to be 3.0 mg/mL in HCT116 cells and 1.7 mg/mL in CT26 cells, respectively (Fig. 2A and B).

We next tested whether Rg3/Rg5-BG induced apoptosis in HCT116 and CT26 cell since apoptosis is a principal form of cellular demise. After being exposed to Rg3/Rg5-BG (3.0 mg/mL) and 5-FU (12.5 μg/mL) for 24 h in HCT116 cells, 5-FU and Rg3/Rg5-BG increased apoptosis rates to 21.92 ± 1.34 % and 16.94 ± 0.30 % respectively, compared to the control value 2.95 ± 0.21 % (Fig. 2C). While in CT26 cells, 5-FU (12.5 μg/mL) and Rg3/Rg5-BG (1.7 mg/mL) increased the apoptosis rates to 12.00 ± 0.65 % and 33.62 ± 3.52 %, respectively, in comparison with the control value 6.27 ± 0.76 % (Fig. 2C). As seen in Fig. 2C, in comparison, with the addition of Rg3/Rg5-BG, the percentage of apoptotic cells (upper-right quadrant) significantly increased, showing late phases of apoptosis occurring in both cells.

To enhance our understanding of the pro-apoptotic effect of Rg3/Rg5-BG, we also conducted cell cycle analysis using flow cytometry. In contrast, we observed a notable reduction in the number of 5-FU-treated HCT116 and CT26 cells in the S phase, a modest reduction in the number of cells in the G2/M phase, accompanied by a substantial increase in the number of cells in the G0/G1 phase (Fig. 2D). Following a 24-h treatment of HCT116 cells with Rg3/Rg5-BG, an increase in the proportion of cells was observed in the G0/G1 phase from 30.69 % to 38.17 %. Meanwhile, the proportion of cells in the S phase decreased slightly from 35.04 % to 26.42 %. Interestingly, the proportion of cells in the G2/M phase remained relatively stable. These results indicated that Rg3/Rg5-BG effectively disrupted the cell cycle of HCT116 cells, causing cell cycle arrest predominantly in the G0/G1 phase. Simultaneously, the G0/G1 ratio of CT26 cells decreased from 42.77 % to 35.90 %, while the G2/M ratio increased from 17.69 % to 24.56 %, which indicated that CT26 cells were effectively blocked in the G2/M phase. Collectively, the results suggest that Rg3/Rg5-BG induces notable disruptions to the cell cycle, leading to an increase in apoptosis in both cells.

3.3. Rg3/Rg5-BG inhibited the growth of CRC xenograft tumors in nude mice

We further investigated the antitumor effects of Rg3/Rg5-BG in vivo. There were no noteworthy differences in body weight between treated and untreated mice (Fig. 3A). Rg3/Rg5-BG inhibited the growth of tumors in nude mice (Fig. 3B). According to Fig. 3C, obviously, mice treated with BG and 5-FU had smaller tumor sizes overall than those in the model group, demonstrating the effectiveness of Rg3/Rg5-BG on anti-colorectal cancer.

We subsequently evaluated CT26 xenograft tumor samples histologically using H&E staining. In Fig. 3D (left column), tumor cells exhibited high proliferation in the model group and comparatively lower proliferation in the Rg3/Rg5-BG and 5-FU treatment groups. Apoptosis induction by Rg3/Rg5-BG in xenograft tumors was also assessed. Compared to the model group, both Rg3/Rg5-BG and 5-FU treatment groups showed significantly higher percentages of TUNEL-positive cells, as depicted in Fig. 3D and E. Overall, inhibition of CRC development by Rg3/Rg5-BG in the xenograft model might be mediated through apoptosis induction.

Besides testing the morphology and pathological results of tumor tissues affected by Rg3/Rg5-BG, we further examined the levels of cytokines IL-2 and TNF-α. As shown in Fig. 4, TNF-α and IL-2 levels were significantly higher in the mouse serum in the Rg3/Rg5-BG and 5-FU groups, indicating enhanced immune function and suppression of tumor cell development via Rg3/Rg5-BG.

3.4. Rg3/Rg5-BG inhibited the malignant progression of CRC by activating Akt

It's well known that apoptosis is regulated by Akt, Bax, Bcl-2, caspase-8 and other signaling pathways (Pistritto et al., 2016). Therefore, next, the effects of Rg3/Rg5-BG on the levels of apoptosis-related proteins in CRC xenograft tumors were detected. As shown in Fig. 5, The Rg3/Rg5-BG treatment led to a reduction in the levels of the anti-apoptotic protein Bcl-2 and p-Akt, alongside increased levels of Bax, caspase-8, and cleaved caspase-3 compared to those in the model group. Furthermore, the administration of Rg3/Rg5-BG resulted in a substantial elevation of the Bax/Bcl-2 ratio. Akt activation promotes cell survival and growth, while its inactivation can halt cellular growth (Vega et al., 2006). Rg3/Rg5-BG significantly reduced p-Akt protein levels, indicating suppression of Akt activation. Based on the aforementioned results, it can be concluded that Rg3/Rg5-BG effectively suppressed the malignant progression of CRC by inhibiting Akt phosphorylation,

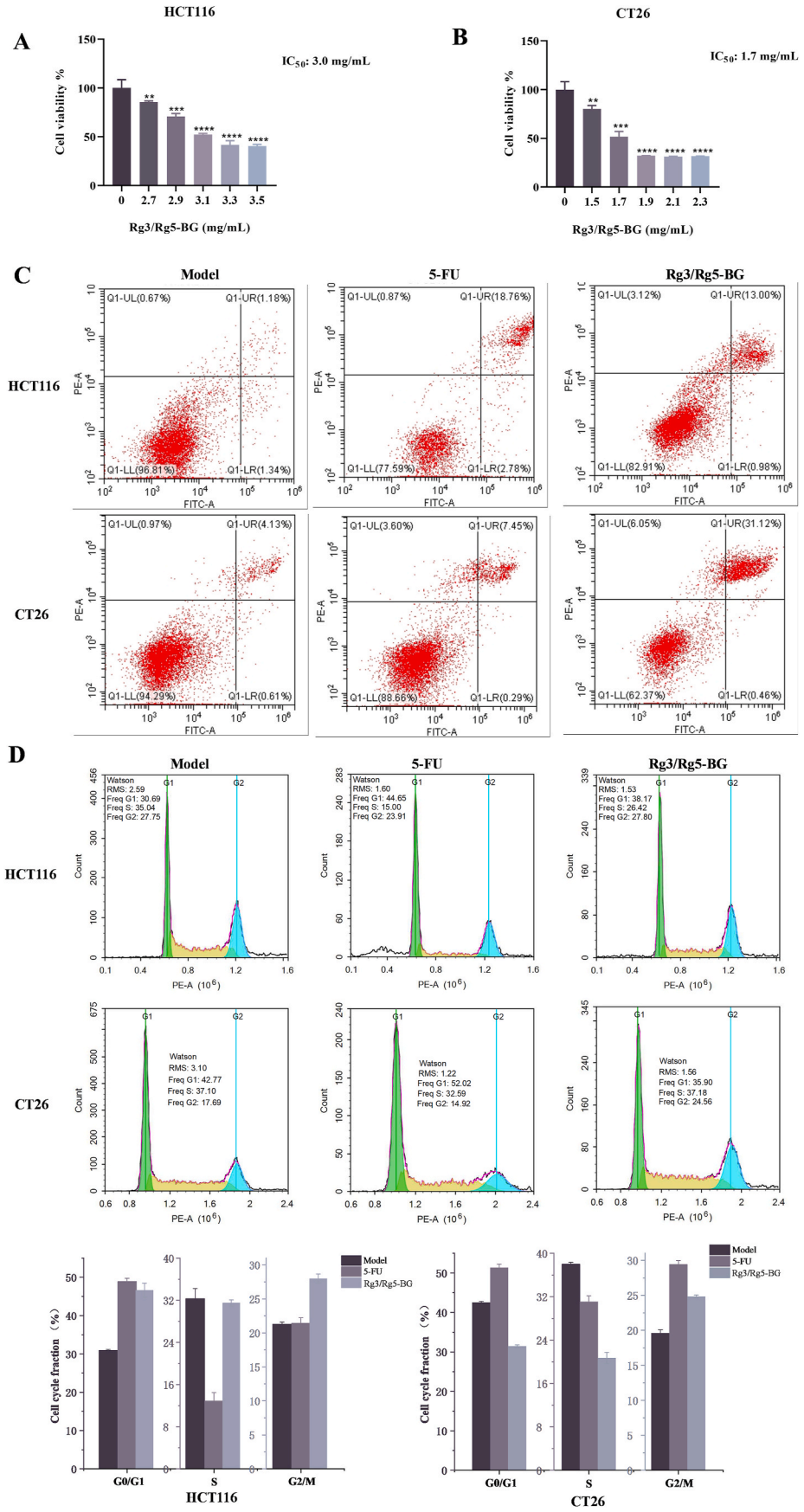

Fig. 2. Viability of (A) HCT116 and (B) CT26 cells treated with Rg3/Rg5-BG. $^{*}p < 0.05$, $^{**}p < 0.01$, $^{***}p < 0.001$ and $^{****}p < 0.0001$ compared with the control group (n = 5). (C) Effect of Rg3/Rg5-BG on apoptosis in HCT116 and CT26 cells. (D) Histograms and bar graphs displaying the cell cycle distribution of HCT116 and CT26 following various treatments (n = 3).

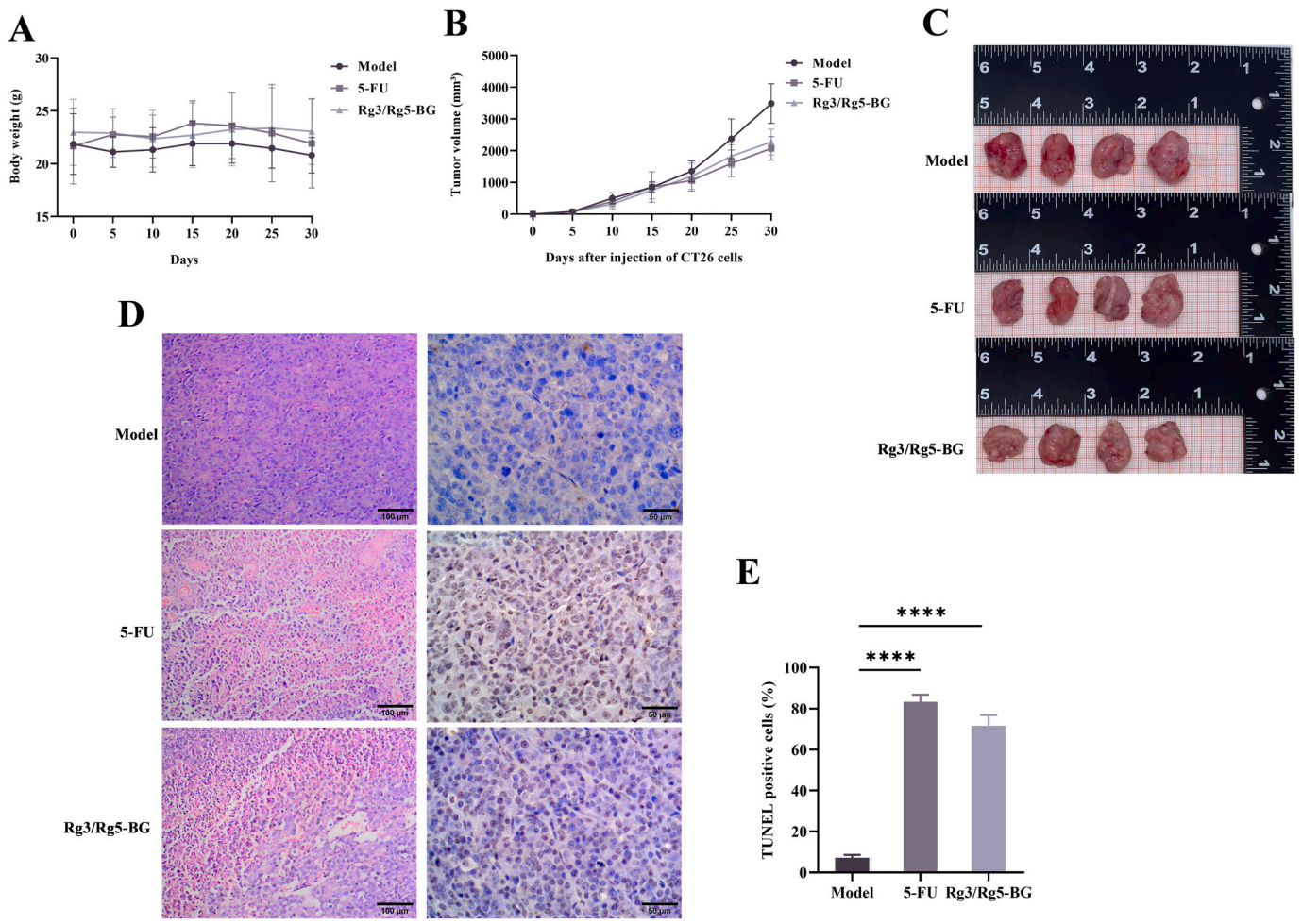

Fig. 3. (A) Body weight and (B) tumor volume changes of mice between treated mice and untreated control during 24 days. (C) Tumor sizes in treated and untreated groups. (D) Histologic and (E) TUNEL staining of Rg3/Rg5-BG-treated colorectal tumors. Tumor samples derived from CT26 xenografts were retrieved, fixed, and paraffin embedded (n = 3). ***$p < 0.001$ and ****$p < 0.0001$.

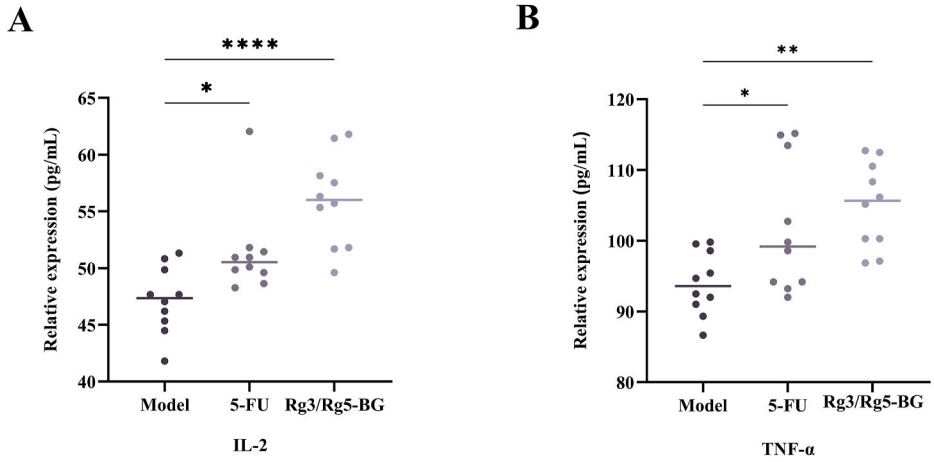

Fig. 4. Effect of Rg3/Rg5-BG on (A) IL-2 and (B) TNF-α levels in CRC mouse sera (n = 6). *$p < 0.05$; **$p < 0.01$, ***$p < 0.001$ and ****$p < 0.0001$.

consequently enhancing the expression of Bax/Bcl-2, and activating caspase-8 and cleaved caspase-3.

3.5. Rg3/Rg5-BG modulated the gut microbiome composition

The effect of Rg3/Rg5-BG on fecal microbiota in CRC mice after 3-week intervention was analyzed (Fig. 6). The Simpson index (diversity index), which was employed to characterize gut microbial alpha diversity, showed that the intestinal microbial species richness in the model group gradually decreased, while, that in the Rg3/Rg5-BG group was partially restored (Fig. 6A). Additionally, as the number of sequencing data constituting the rarefaction curves rose, more species

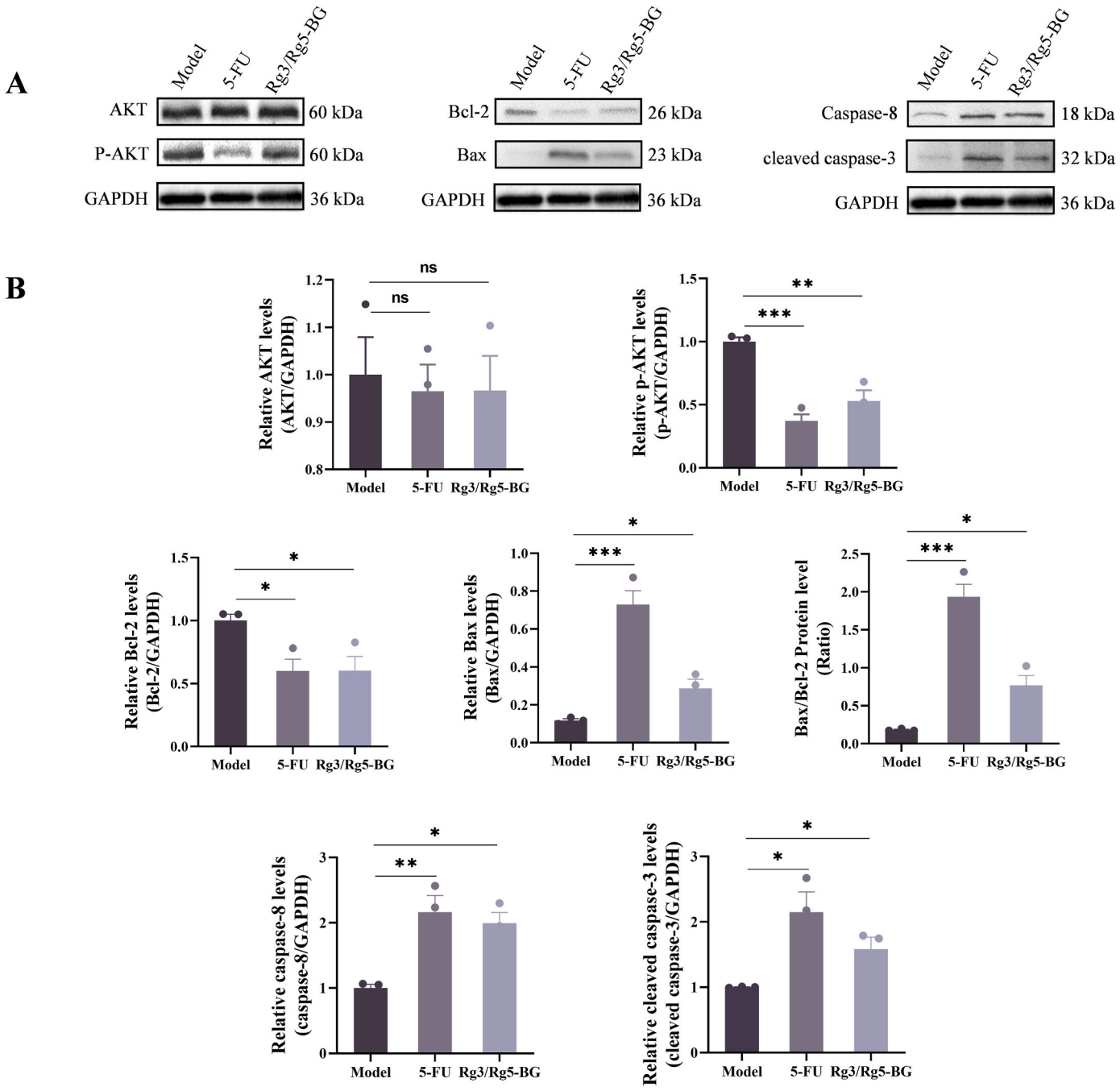

Fig. 5. (A) Representative WB results of p-AKT, AKT, Bax, Bcl-2, caspase-8, cleaved caspase-3, and GAPDH in CRC xenograft tumors. (B) Quantification of the corresponding protein levels normalized to GAPDH (n = 3). *$p < 0.05$; **$p < 0.01$, ***$p < 0.001$ and ****$p < 0.0001$.

were observed (Fig. 6B). The rarefaction curve seemed to stabilize once the volume of sequencing data reached a particular threshold, indicating that gut microbial diversity gradually increased. The beta diversity analysis through principal coordinate analysis (PCoA) unveiled a clear distinction in the clustering of gut microbiota composition between the two groups (Fig. 6C). To explore possible correlations between tumor multiplicity and variations in bacterial colonization, we examined the bacterial communities present in stool samples. The total intestinal flora distribution between the two groups varied, as depicted in Fig. 6D. Next, we used the linear discriminant analysis effect size (LEfSe) tool on the I-Sanger platform to search specialized communities in samples. LDA scores in Fig. 6E indicated differentially abundant taxa between the two groups. The contribution of specific bacteria was shown by the length of the bar in the bar chart. At the phylum level (Fig. 6F), the relative abundance of *Candidatus_Saccharibacteria* was significantly higher in the Rg3/Rg5-BG group compared to the CRC model group. As shown in Fig. 6G, the genus-level taxonomic microbiota composition mainly included *Vampirovibrio*, *Mobilitalea*, and *Peptococcus*. The relative abundances significantly decreased in *Vampirovibrio*, *Clostridium_XlVb*, *Acetatifactor*, *Mobilitalea*, and *Peptococcus* but significantly increased in *Saccharibacteria_genera_incertae_sedis* in the Rg3/Rg5-BG-treated group versus the model group ($P < 0.05$).

Functional changes in the intestinal microbiome of CRC mice were assessed using the PICRUSt2 method with the COG and KEGG databases (Fig. 7A and B). Metabolic pathways and functions of the gut microbiome in both groups were markedly enhanced, including “Aspartate 1-decarboxylase”, “Isopentenyldiphosphate isomerase”, “Glutamate-1-semialdehyde aminotransferase”, “Transposase” and more (Fig. 7C). We

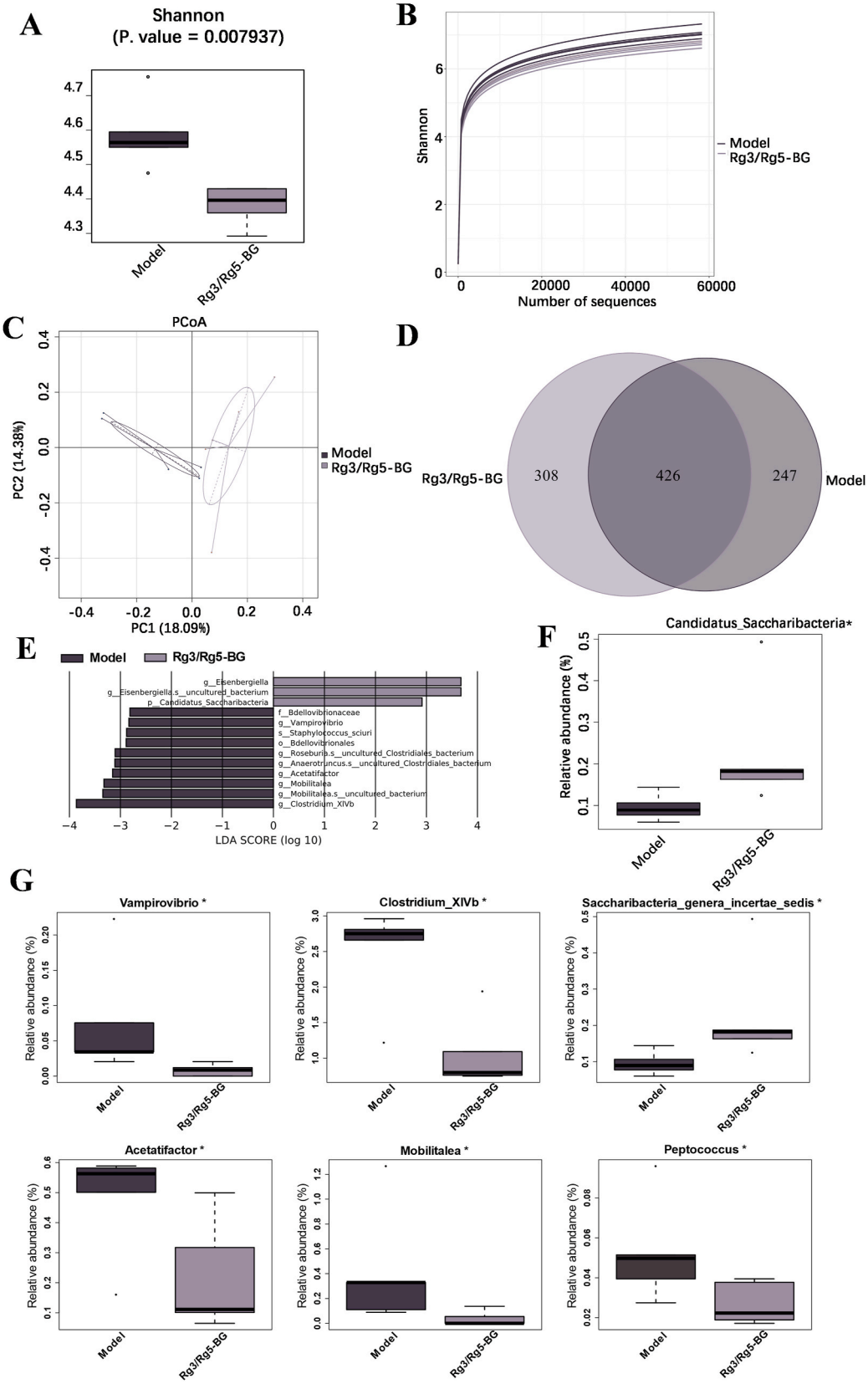

Fig. 6. (A) The Simpson index revealed significant disparities between the two groups. (B) Rarefaction curves calculated from the fora sequencing data using the Sobs index of the OTU level. (C) PCoA of beta diversity calculated on the weighted UniFrac distances using OTU data at the phylum level of mice in the two groups. (D) Number of species of bacterial taxa of mice in two groups. (E) Discriminative taxa determined by LEfSe of the gut microbiota from mice in $\log_{10}$ LDA >2.0. (F) Relative abundance of significantly altered gut bacteria at the phylum level in mice. (G) Comparison of the relative abundance of bacterial taxa at the genus level. Data are presented as the mean ± SD (n = 3). n = 3, $^{*}p < 0.05$; $^{**}p < 0.01$.

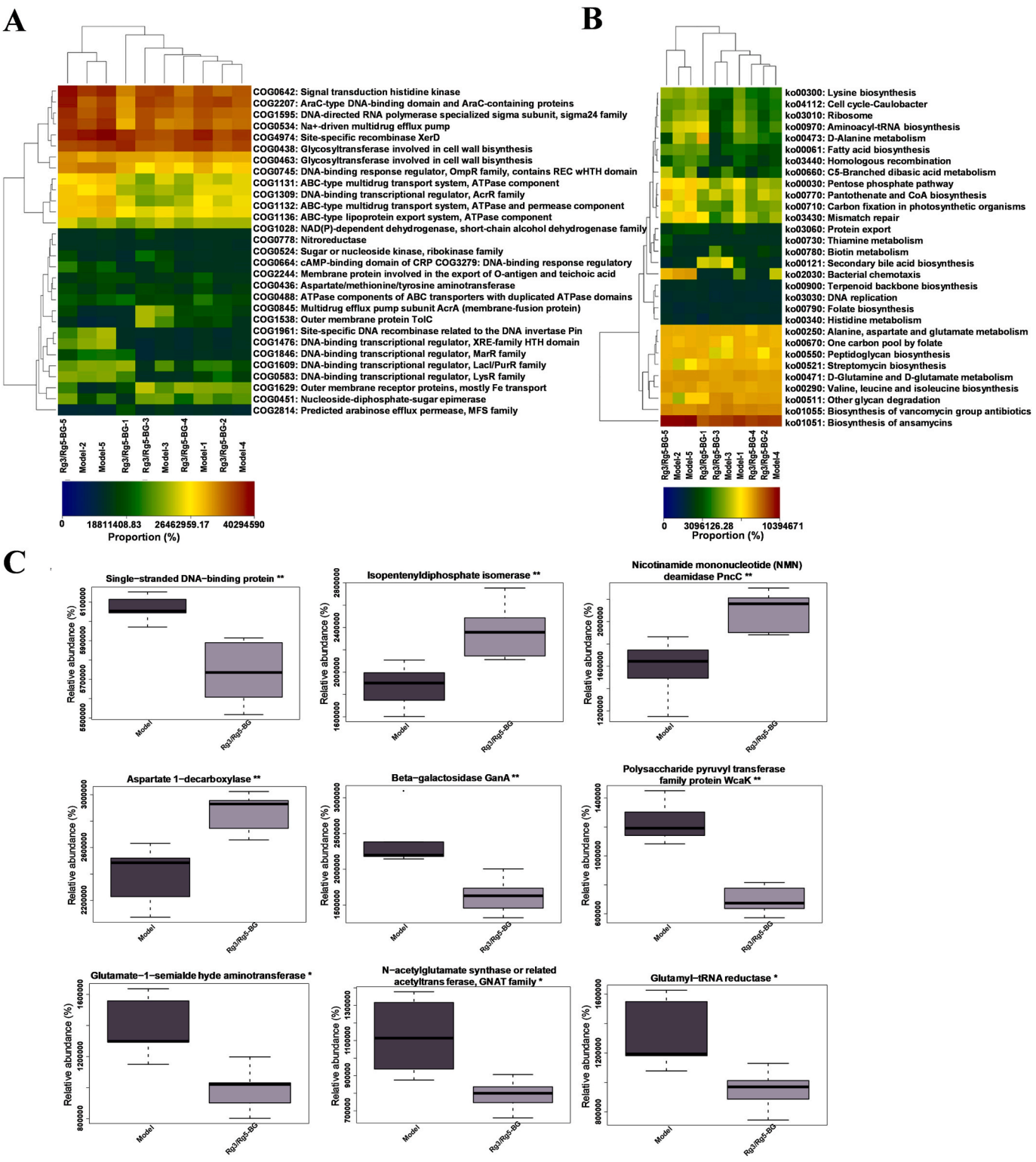

Fig. 7. (A) A heatmap displays enriched COG pathways, with the top 30 pathways indicating differences in abundance among groups. (B) A heatmap displays enriched KEGG pathways, with the top 30 pathways indicating differences in abundance among groups. The figure shows a color gradient from light to dark representing a relative abundance from low to high. (C) COG pathways and KEGG pathways exhibiting significant differences between the two groups were identified. Statistical significance was denoted as follows: $*p < 0.05$; $**p < 0.01$.

infer that the biochemical mechanisms listed above may play key roles in cell proliferation and differentiation.

4. Discussion

Some publications have linked ginsenosides in black ginseng to cancer (Chen et al., 2017; Pistritto et al., 2016; Vega et al., 2006; Wei et al., 2023; Zhang et al., 2024), while this is the first study to

demonstrate that the total ginsenosides from black ginseng, innovatively prepared by low temperature steam-heating process, inhibited CRC tumor growth by activating the Akt/Bax/caspase-3 pathway and modulating gut microbiota. Prior work has demonstrated that black ginseng has more potent biological and pharmacological activities, for example, inhibitory effect on various cancers, than white and red ginseng (Kang et al., 2015; Metwaly et al., 2019). To the best of our knowledge, there are few reports regarding the inhibition of CRC tumor growth by BG. BG extract prepared with 70 % ethanol showed significantly greater inhibitory effect on colon26-M3.1 carcinoma cells than that of white ginseng (Kim et al., 2010). The ginsenoside extract of BG exhibited significantly stronger cytotoxic effects compared to the RG extract in the CRC cancer cell line (HT-29), with its efficacy closely resembling that of ginsenoside Rg5 (Park et al., 2022). To date, there is a lack of in vivo research regarding the effects of ginsenoside extracts from BG on CRC.

A substantial amount of evidence suggests that rare ginsenosides can exert anti-cancer effects (Hong et al., 2021; Huang et al., 2022; Valdés-González et al., 2023; Wang et al., 2021; Zhao et al., 2022). In the present study, the contents of rare ginsenosides were much higher in black ginseng than those in red ginseng (Fig. 1). Our data provide the initial evidence suggesting that Rg3/Rg5-BG may exhibit superior anticancer properties. In this vein, we described a specific increase in apoptosis in both CRC cell lines, by Rg3/Rg5-BG intervention (Fig. 2A–D). Using flow cytometry, we observed that Rg3/Rg5-BG effectively triggered apoptosis in HCT116 cells and halted cell cycle progression at the G0/G1 phase, which is consistent with the previous report (Kim and Kim, 2015). The G1 phase of the cell cycle is vital for regulating cell proliferation and differentiation (Hall and Peters, 1996). Thus, pharmaceuticals capable of inducing G1 phase cell cycle arrest possess the potential to regulate cellular differentiation and progression throughout the carcinogenic process. Furthermore, our data also suggested that the effects of Rg3/Rg5-BG on CT26 CRC cells resulted in cell arrest, more precisely in the G2/M arrest. Notably, the same phase result has been yielded in the ginseng berry concentrate experiment (Wang et al., 2021). It was obvious that Rg3/Rg5-BG-induced cell cycle arrest varied between cell lines.

In our in vivo study, Rg3/Rg5-BG also had an anti-cancer effect by causing tumor cell death and decreasing tumor size in CT26 CRC -bearing mice (Fig. 3A–E), which is in good agreement with the previous reports that black ginseng has demonstrated anti-cancer properties by reducing the size and volume of solid tumors in various animal studies (Kang et al., 2015). Further, we observed that Rg3/Rg5-BG intervention in CRC mice significantly up-regulated TNF-α and IL-2 levels (Fig. 4A and B), which can promote apoptosis and play an anti-tumor role (Mann, 2002; Taga et al., 1999). Collectively, the present study linked Rg3/Rg5-BG to CRC, perhaps precipitated by abundant rare ginsenosides observed in the BG processed by the innovative approach.

Cancer cells evade apoptosis by enhancing antiapoptotic genes such as Bcl-2, and Akt, while suppressing pro-apoptotic proteins including Bax, caspase family members, thus disrupting and implicating defective apoptosis (Ashkenazi and Dixit, 1998; Gonçalves et al., 2021; Green and Kroemer, 2004; Lu et al., 2018). In this context, the mechanism by which Rg3/Rg5-BG induces apoptosis in tumor cells has been elucidated (Fig. 8), as evidenced by significantly increased expression of anti-apoptotic members Bax, caspase-8, and cleaved caspase-3, decreased expression of Bcl-2 in the Rg3/Rg5-BG-treated mice (Fig. 5). It was deduced that both the Bax/Bcl-2 complex and caspase-8 led to the activation of caspase-3, a critical effector in apoptosis (Ashkenazi and Dixit, 1998).

Regulation of apoptosis via AKT, which plays a crucial role in tumorigenesis (Xia et al., 2020), extends to key downstream targets such as Bax/Bcl-2 and caspase-8/caspase-3 (Simonyan et al., 2016; Yuan et al., 2019). In this study, the Bax/Bcl-2 ratio in the Rg3/Rg5-BG group was markedly elevated compared to that in the model group, meanwhile Rg3/Rg5-BG effectively reduced p-AKT protein expression (Fig. 5B), suggesting that the Rg3/Rg5-BG-induced Bax/caspase-3 cascade response may be dependent on the blockage of the Akt pathway (Fig. 8). Encouragingly, in this study, we made a significant discovery regarding the potential of total ginsenosides in BG to restrain the malignant progression of CRC.

Gut microbiota dysbiosis is implicated in CRC development and progression (Ekiert and Szopa, 2020; Yu et al., 2017). Our research unveiled that the supplementation of Rg3/Rg5-BG improved the equilibrium of the intestinal microbiota (Fig. 6G). Rg3/Rg5-BG contributed to balance the ecological imbalances in CRC, which may lead to cancer

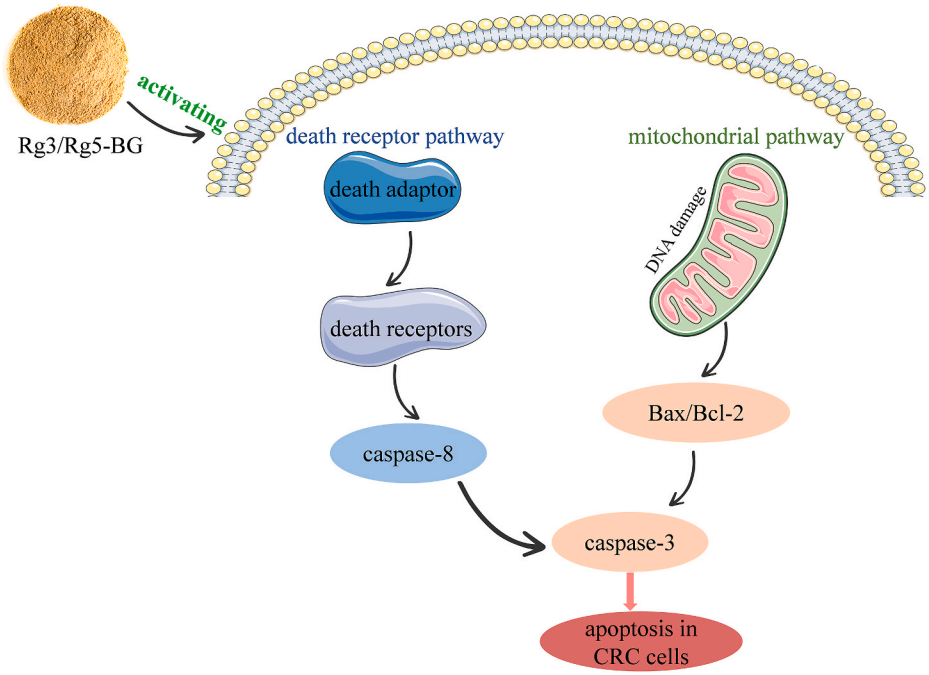

Fig. 8. The potential mechanism of Rg3/Rg5-BG in the treatment of CRC by activating Akt/Bax/caspase-3 pathway using the HTC116 and CT26 cell lines.

remission. Furthermore, the gut microbiota contributes to metabolic functions (Boleij and Tjalsma, 2012). Interestingly, we observed that Rg3/Rg5-BG regulated some metabolic pathways in Fig. 7A–C, which can affect gene expression, differentiation, and proliferation of intestinal epithelial cells (Park et al., 2022; Wong and Yu, 2023). The results suggest that the anti-cancer efficacy of Rg3/Rg5-BG may, in part, be ascribed to its influence on gut population modulation.

5. Conclusions

Our research demonstrated that Rg3/Rg5-BG significantly reduced the viability of HCT116 and CT26 cells, primarily through mechanisms of cell cycle arrest and apoptosis. In vivo, Rg3/Rg5-BG effectively inhibits Akt phosphorylation upstream, thereby modulating the death receptor and mitochondrial pathways crucially involved in apoptosis. In conclusion, Rg3/Rg5-BG can maintain the homeostasis of the body, promote the secretion of apoptotic factors in cancer cells, regulate the intestinal microbiota, and interfere with tumor growth. Thus, Rg3/Rg5-BG has great potential as a natural drug for promoting the treatment and management of colorectal cancer. In the long run, our study plays a cornerstone role in understanding the integrated system of natural products in cancer treatment.

CRediT authorship contribution statement

Peng Yu: Investigation, Methodology, Writing – original draft. **Weiyin Xu:** Investigation, Validation, Data statistic. **Yanqi Li:** Investigation. **Zhaoyang Xie:** Revision. **Simeng Shao:** Data statistic. **Jianing Liu:** Revision. **Ying Wang:** Investigation. **Long Wang:** Writing – review & editing. **Hongmei Yang:** Methodology, Supervision, Writing – review & editing.

Declaration of competing interest

The authors declare that they have no known competing financial interests or personal relationships that could have appeared to influence the work reported in this paper.

Acknowledgements

This work was supported by the Science and Technology Development Planning Project of Jilin Province (no. YDZJ202401426ZYTS) and Project for Outstanding Young Scientific and Technological Talents of Changchun University of Chinese Medicine (no. 2024JQ02). We extend our gratitude to Genesky Biotechnology (Shanghai, China) for their exceptional technical support in the analysis of 16S ribosomal DNA sequencing.

Data availability

Data will be made available on request.

References

Ashkenazi, A., Dixit, V.M., 1998. Death receptors: signaling and modulation. Science 281 (5381), 1305–1308. https://doi.org/10.1126/science.281.5381.1305.

Boleij, A., Tjalsma, H., 2012. Gut bacteria in health and disease: a survey on the interface between intestinal microbiology and colorectal cancer. Biol. Rev. Camb. Phil. Soc. 87 (3), 701–730. https://doi.org/10.1111/j.1469-185X.2012.00218.x.

Brenner, H., Kloor, M., Pox, C.P., 2014. Colorectal cancer. Lancet 383 (9927), 1490–1502. https://doi.org/10.1016/S0140-6736(13)61649-9.

Chen, G., Li, H., Gao, Y., Zhang, L., Zhao, Y., 2017. Flavored black ginseng exhibited antitumor activity via improving immune function and inducing apoptosis. Food Funct. 8 (5), 1880–1889. https://doi.org/10.1039/c6fo01870j.

Chen, L., Brar, M.S., Leung, F.C., Hsiao, W.L., 2016. Triterpenoid herbal saponins enhance beneficial bacteria, decrease sulfate-reducing bacteria, modulate inflammatory intestinal microenvironment and exert cancer preventive effects in ApcMin/+ mice. Oncotarget 7 (21), 31226–31242. https://doi.org/10.18632/oncotarget.8886.

Ekiert, H.M., Szopa, A., 2020. Biological activities of natural products. Molecules 25 (23). https://doi.org/10.3390/molecules25235769.

Focaccetti, C., Bruno, A., Magnani, E., Bartolini, D., Principi, E., Dallaglio, K., Bucci, E.O., Finzi, G., Sessa, F., Noonan, D.M., Albini, A., 2015. Effects of 5-fluorouracil on morphology, cell cycle, proliferation, apoptosis, autophagy and ROS production in endothelial cells and cardiomyocytes. PLoS One 10 (2), e0115686. https://doi.org/10.1371/journal.pone.0115686.

Gagnière, J., Raisch, J., Veziant, J., Barnich, N., Bonnet, R., Buc, E., Bringer, M.A., Pezet, D., Bonnet, M., 2016. Gut microbiota imbalance and colorectal cancer. World J. Gastroenterol. 22 (2), 501–518. https://doi.org/10.3748/wjg.v22.i2.501.

Gonçalves, A.C., Richiardone, E., Jorge, J., Polónia, B., Xavier, C.P.R., Salaroglio, I.C., Riganti, C., Vasconcelos, M.H., Corbet, C., Sarmento-Ribeiro, A.B., 2021. Impact of cancer metabolism on therapy resistance-Clinical implications. Drug Resist. Updates 59, 100797. https://doi.org/10.1016/j.drup.2021.100797.

Green, D.R., Kroemer, G., 2004. The pathophysiology of mitochondrial cell death. Science 305 (5684), 626–629. https://doi.org/10.1126/science.1099320.

Hall, M., Peters, G., 1996. Genetic alterations of cyclins, cyclin-dependent kinases, and Cdk inhibitors in human cancer. Adv. Cancer Res. 68, 67–108. https://doi.org/10.1016/s0065-230x(08)60352-8.

He, B.C., Gao, J.L., Luo, X., Luo, J., Shen, J., Wang, L., Zhou, Q., Wang, Y.T., Luu, H.H., Haydon, R.C., Wang, C.Z., Du, W., Yuan, C.S., He, T.C., Zhang, B.Q., 2011. Ginsenoside Rg3 inhibits colorectal tumor growth through the down-regulation of Wnt/ß-catenin signaling. Int. J. Oncol. 38 (2), 437–445. https://doi.org/10.3892/ijo.2010.858.

Hong, H., Baatar, D., Hwang, S.G., 2021. Anticancer activities of ginsenosides, the main active components of ginseng. Evid Based Complement Alternat Med, 8858006. https://doi.org/10.1155/2021/8858006, 2021.

Huang, J., Liu, D., Wang, Y., Liu, L., Li, J., Yuan, J., Jiang, Z., Jiang, Z., Hsiao, W.W., Liu, H., Khan, I., Xie, Y., Wu, J., Xie, Y., Zhang, Y., Fu, Y., Liao, J., Wang, W., Lai, H., Shi, A., Cai, J., Luo, L., Li, R., Yao, X., Fan, X., Wu, Q., Liu, Z., Yan, P., Lu, J., Yang, M., Wang, L., Cao, Y., Wei, H., Leung, E.L., 2022. Ginseng polysaccharides alter the gut microbiota and kynurenine/tryptophan ratio, potentiating the antitumour effect of antiprogrammed cell death 1/programmed cell death ligand 1 (anti-PD-1/PD-L1) immunotherapy. Gut 71 (4), 734–745. https://doi.org/10.1136/gutjnl-2020-321031.

Huang, L., Li, H.J., Wu, Y.C., 2023. Processing technologies, phytochemistry, bioactivities and applications of black ginseng-a novel manufactured ginseng product: a comprehensive review. Food Chem. 407, 134714. https://doi.org/10.1016/j.foodchem.2022.134714.

Jin, Y., Kim, Y.J., Jeon, J.N., Wang, C., Min, J.W., Noh, H.Y., Yang, D.C., 2015. Effect of white, red and black ginseng on physicochemical properties and ginsenosides. Plant Foods Hum. Nutr. 70 (2), 141–145. https://doi.org/10.1007/s11130-015-0470-0.

Kang, S.J., Han, J.S., Kim, A., 2015. Ameliorate effect of black ginseng on HepG2 cell transplanted in BALB/c nude mice. Kor. J. Food Nutr. 28, 241–246. https://doi.org/10.9799/ksfan.2015.28.2.241.

Kim, A.J., Kang, S.J., Lee, K.H., Lee, M., Ha, S.D., Cha, Y.S., Kim, S.Y., 2010. The chemopreventive potential and anti-inflammatory activities of Korean black ginseng in colon26-M3.1 carcinoma cells and macrophages. J Korean Soc Appl Biol Chem. 53 (1), 101–105. https://doi.org/10.3839/jksabc.2010.017.

Kim, S.J., Kim, A.K., 2015. Anti-breast cancer activity of fine black ginseng (Panax ginseng Meyer) and ginsenoside Rg5. J Ginseng Res 39 (2), 125–134. https://doi.org/10.1016/j.jgr.2014.09.003.

Liu, T., Duo, L., Duan, P., 2018. Ginsenoside Rg3 sensitizes colorectal cancer to radiotherapy through downregulation of proliferative and angiogenic biomarkers. Evid Based Complement Alternat Med, 1580427. https://doi.org/10.1155/2018/1580427, 2018.

Lu, C., Wang, Y., Xu, T., Li, Q., Wang, D., Zhang, L., Fan, B., Wang, F., Liu, X., 2018. Genistein ameliorates scopolamine-induced amnesia in mice through the regulation of the cholinergic neurotransmission, antioxidant system and the ERK/CREB/BDNF signaling. Front. Pharmacol. 9, 1153. https://doi.org/10.3389/fphar.2018.01153.

Mann, J., 2002. Natural products in cancer chemotherapy: past, present and future. Nat. Rev. Cancer 2 (2), 143–148. https://doi.org/10.1038/nrc723.

Metwaly, A.M., Lianlian, Z., Luqi, H., Deqiang, D., 2019. Black Ginseng and its saponins: preparation, phytochemistry and pharmacological effects. Molecules 24 (10). https://doi.org/10.3390/molecules24101856.

Miller, K.D., Siegel, R.L., Lin, C.C., Mariotto, A.B., Kramer, J.L., Rowland, J.H., Stein, K. D., Alteri, R., Jemal, A., 2016. Cancer treatment and survivorship statistics, 2016. Ca - Cancer J. Clin. 66 (4), 271–289. https://doi.org/10.3322/caac.21349.

Park, E.M., Chelvanambi, M., Bhutiani, N., Kroemer, G., Zitvogel, L., Wargo, J.A., 2022. Targeting the gut and tumor microbiota in cancer. Nat. Med. 28 (4), 690–703. https://doi.org/10.1038/s41591-022-01779-2.

Park, J.S., Kim, S.H., Han, K.M., Kim, Y.S., Kwon, E., Paek, S.H., Seo, Y.K., Yun, J.W., Kang, B.C., 2022. Efficacy and safety evaluation of black ginseng (Panax ginseng C. A. Mey.) extract (CJ EnerG): broad spectrum cytotoxic activity in human cancer cell lines and 28-day repeated oral toxicity study in Sprague-Dawley rats. BMC Complement Med Ther 22 (1), 44. https://doi.org/10.1186/s12906-022-03522-3.

Phi, L.T.H., Wijaya, Y.T., Sari, I.N., Yang, Y.G., Lee, Y.K., Kwon, H.Y., 2018. The anti-metastatic effect of ginsenoside Rb2 in colorectal cancer in an EGFR/SOX2-dependent manner. Cancer Med. 7 (11), 5621–5631. https://doi.org/10.1002/cam4.1800.

Pistritto, G., Trisciuoglio, D., Ceci, C., Garufi, A., D'Orazi, G., 2016. Apoptosis as anticancer mechanism: function and dysfunction of its modulators and targeted therapeutic strategies. Aging 8 (4), 603–619. https://doi.org/10.18632/aging.100934.

Saeed, M.M., Fernández-Ochoa, Á., Saber, F.R., Sayed, R.H., Cádiz-Gurrea, M.L., Elmotayam, A.K., Leyva-Jiménez, F.J., Segura-Carretero, A., Nadeem, R.I., 2022. The

potential neuroprotective effect of Cyperus Esculentus L. extract in scopolamine-induced cognitive impairment in rats: extensive biological and metabolomics approaches. Molecules 27 (20). https://doi.org/10.3390/molecules27207118.

Siegel, R.L., Miller, K.D., Jemal, A., 2019. Cancer statistics, 2019. Ca - Cancer J. Clin. 69 (1), 7–34. https://doi.org/10.3322/caac.21551.

Simonyan, L., Renault, T.T., Novais, M.J., Sousa, M.J., Côrte-Real, M., Camougrand, N., Gonzalez, C., Manon, S., 2016. Regulation of Bax/mitochondria interaction by AKT. FEBS Lett. 590 (1), 13–21. https://doi.org/10.1002/1873-3468.12030.

Taga, K., Yamauchi, A., Bloom, E.T., 1999. Target cell-induced apoptosis in IL-2-activated human natural killer cells. Leuk. Lymphoma 32 (5–6), 451–458. https://doi.org/10.3109/10428199909058402.

Tilg, H., Adolph, T.E., Gerner, R.R., Moschen, A.R., 2018. The intestinal microbiota in colorectal cancer. Cancer Cell 33 (6), 954–964. https://doi.org/10.1016/j.ccell.2018.03.004.

Valdés-González, J.A., Sánchez, M., Moratilla-Rivera, I., Iglesias, I., Gómez-Serranillos, M.P., 2023. Immunomodulatory, anti-inflammatory, and anti-cancer properties of ginseng: a pharmacological update. Molecules 28 (9). https://doi.org/10.3390/molecules28093863.

Vega, F., Medeiros, L.J., Leventaki, V., Atwell, C., Cho-Vega, J.H., Tian, L., Claret, F.X., Rassidakis, G.Z., 2006. Activation of mammalian target of rapamycin signaling pathway contributes to tumor cell survival in anaplastic lymphoma kinase-positive anaplastic large cell lymphoma. Cancer Res. 66 (13), 6589–6597. https://doi.org/10.1158/0008-5472.Can-05-3018.

Wang, C.Z., Wan, C., Luo, Y., Zhang, C.F., Zhang, Q.H., Chen, L., Park, C.W., Kim, S.H., Liu, Z., Lager, M., Xu, M., Hou, L., Yuan, C.S., 2021. Ginseng berry concentrate prevents colon cancer via cell cycle, apoptosis regulation, and inflammation-linked Th17 cell differentiation. J. Physiol. Pharmacol. 72 (2). https://doi.org/10.26402/jpp.2021.2.08.

Wei, W., Liu, X., Tao, Y., Wang, Y., Gong, J., Liu, S., 2023. Saponin composition comparison of black ginseng and white ginseng by liquid chromatography-mass spectrometry combined with multivariate statistical analysis. Nat. Prod. Res. 37 (19), 3297–3301. https://doi.org/10.1080/14786419.2022.2062352.

Wong, C.C., Yu, J., 2023. Gut microbiota in colorectal cancer development and therapy. Nat. Rev. Clin. Oncol. 20 (7), 429–452. https://doi.org/10.1038/s41571-023-00766-x.

Xia, T., Zhang, J., Zhou, C., Li, Y., Duan, W., Zhang, B., Wang, M., Fang, J., 2020. 20(S)-Ginsenoside Rh2 displays efficacy against T-cell acute lymphoblastic leukemia through the PI3K/Akt/mTOR signal pathway. J Ginseng Res 44 (5), 725–737. https://doi.org/10.1016/j.jgr.2019.07.003.

Yang, J., Yuan, D., Xing, T., Su, H., Zhang, S., Wen, J., Bai, Q., Dang, D., 2016. Ginsenoside Rh2 inhibiting HCT116 colon cancer cell proliferation through blocking PDZ-binding kinase/T-LAK cell-originated protein kinase. J Ginseng Res. 40 (4), 400–408. https://doi.org/10.1016/j.jgr.2016.03.007.

Yu, J., Feng, Q., Wong, S.H., Zhang, D., Liang, Q.Y., Qin, Y., Tang, L., Zhao, H., Stenvang, J., Li, Y., Wang, X., Xu, X., Chen, N., Wu, W.K., Al-Aama, J., Nielsen, H.J., Kiilerich, P., Jensen, B.A., Yau, T.O., Lan, Z., Jia, H., Li, J., Xiao, L., Lam, T.Y., Ng, S. C., Cheng, A.S., Wong, V.W., Chan, F.K., Xu, X., Yang, H., Madsen, L., Datz, C., Tilg, H., Wang, J., Brünner, N., Kristiansen, K., Arumugam, M., Sung, J.J., Wang, J., 2017. Metagenomic analysis of faecal microbiome as a tool towards targeted non-invasive biomarkers for colorectal cancer. Gut 66 (1), 70–78. https://doi.org/10.1136/gutjnl-2015-309800.

Yuan, J., Deng, Y., Zhang, Y., Gan, X., Gao, S., Hu, H., Hu, S., Hu, J., Liu, H., Li, L., Wang, J., 2019. Bmp4 inhibits goose granulosa cell apoptosis via PI3K/AKT/Caspase-9 signaling pathway. Anim. Reprod. Sci. 200, 86–95. https://doi.org/10.1016/j.anireprosci.2018.11.014.

Yun, T.K., Choi, S.Y., 1998. Non-organ specific cancer prevention of ginseng: a prospective study in Korea. Int. J. Epidemiol. 27 (3), 359–364. https://doi.org/10.1093/ije/27.3.359.

Zhang, Y., Huang, Y., Dou, D., 2024. Anti-prostate cancer mechanism of black ginseng during the "nine steaming and nine sun-drying" process based on HPLC analysis combined with vector space network pharmacology. Discov Oncol 15 (1), 12. https://doi.org/10.1007/s12672-024-00862-z.

Zhao, L., Zhang, Y., Li, Y., Li, C., Shi, K., Zhang, K., Liu, N., 2022. Therapeutic effects of ginseng and ginsenosides on colorectal cancer. Food Funct. 13 (12), 6450–6466. https://doi.org/10.1039/D2FO00899H.

Zhu, L., Luan, X., Dou, D., Huang, L., 2019. Comparative analysis of ginsenosides and oligosaccharides in white ginseng (WG), red ginseng (RG) and black ginseng (BG). J. Chromatogr. Sci. 57 (5), 403–410. https://doi.org/10.1093/chromsci/bmz004.